ARTICLE

Influence of Thermal Treatments on In-depth Compositional Uniformity of $CuIn(S,Se)_2$ Thin Films

Hai-bing Xie, Wei-feng Liu*, Guo-shun Jiang, Xin-yi Li, Fei Yan, Chang-fei Zhu*

CAS Key Laboratory of Materials for Energy Conversion, Department of Materials Science and Engineering, University of Science and Technology of China, Hefei 230026, China

(Dated: Received on May 30, 2012; Accepted on June 7, 2012)

$CuIn(S,Se)_2$ thin films were prepared by thermal crystallization of co-sputtered Cu-In alloy precursors in S/Se atmosphere. In-depth compositional uniformity is an important prerequisite for obtaining device-quality $CuIn(S,Se)_2$ absorber thin films. In order to figure out the influence of heat treatments on in-depth composition uniformity of $CuIn(S,Se)_2$ thin films, two kinds of reaction temperature profiles were investigated. One process is "one step profile", referring to formation of $CuIn(S,Se)_2$ thin films just at elevated temperature (*e.g.* 500 °C). The other is "two step profile", which allows for slow diffusion of S and Se elements into the alloy precursors at a low temperature before the formation and re-crystallization of $CuIn(S,Se)_2$ thin films at higher temperature (*e.g.* first 250 °C then 500 °C). X-ray diffraction studies reveal that there is a discrepancy in the shape of (112) peak. Samples annealed with "one step profile" have splits on (112) peaks, while samples annealed with "two step profile" have relatively symmetrical (112) peaks. Grazing incident X-ray diffraction and energy dispersive spectrum measurements of samples successively etched in bromine methanol show that $CuIn(S,Se)_2$ thin films have better in-depth composition uniformity after "two step profile" annealing. The reaction mechanism during the two thermal processing was also investigated by X-ray diffraction and Raman spectra.

Key words: Thermal treatment, In-depth compositional uniformity, $CuIn(S,Se)_2$ thin film

I. INTRODUCTION

$CuInSe_2$ based thin film solar cells are very attractive and promising for next generation photovoltaic devices, due to a very high absorption coefficient (10^4–10^5 cm^{-1}) and near zero degradation of the cell performance. However, the band gap of $CuInSe_2$ is only 1.04 eV, lower than the optimal band of 1.4 eV which is considered to theoretically match the optimum for conversion of the solar spectrum. Band gap optimization is typically achieved by partially substituting indium (In) or selenium (Se) with gallium (Ga) or sulfur (S), to form $Cu(In,Ga)Se_2$ or $CuIn(S,Se)_2$ thin films, respectively. Solar cells based on $Cu(In,Ga)Se_2$ have already attained a conversion efficiency of 20.3% by Jackson *et al.* in ZSW [1]. For $CuIn(S,Se)_2$ thin film, it is easy to tune band gap from 1.04 eV to 1.54 eV by changing S/(S+Se) ratio in the films. In addition, selenium is toxic and not very safe for solar cell production, partially replacing Se with S will be advantageous for production and environment. The main problem to prepare $CuIn(S,Se)_2$ films is separation or at least partial separation of the ternary phases of $CuInSe_2$ and $CuInS_2$ [2]. Several researchers have reported the preparation and characterization of $CuIn(S,Se)_2$ films in different technological routes. Alberts *et al.* have reported deposition of homogeneous $CuIn(Se,S)_2$ thin films by sulfurization of selenized Cu/In alloys in Ar/H_2S [2]. The most critical aspect of this technology was related to the manipulation of the selenization conditions to promote the partial formation of $CuInSe_2$. Fully formation of $CuInSe_2$ before sulfurization caused phase separation. Bandyopadhyaya *et al.* have achieved homogeneous $CuIn(S,Se)_2$ films by sulphurization of In/Cu stacked elemental layers in S vapor followed by selenization in graphite box in Se vapor [3]. It was easier for Se substitution of S due to the lower formation energy of $CuInSe_2$ compared to that of $CuInS_2$, so the thermo-dynamical formation of $CuInSe_2$ was favored. Preparation of $CuIn(S,Se)_2$ thin films by simultaneous thermal crystallization of Cu-In-S or Cu-In-Se containing precursors in sulfur and selenium atmosphere was reported by Yamaguchi *et al.* [4, 5]. Adurodija *et al.* have synthesized $CuIn(S,Se)_2$ thin films by thermal diffusion of sulfur and selenium vapors into co-sputtered Cu-In alloy within a closed graphite container [6]. However, few results about the compositional uniformity of $CuIn(S,Se)_2$ thin films by simultaneous sufo-selenization methods were presented.

In this work, formation of $CuIn(S,Se)_2$ thin films by

*Authors to whom correspondence should be addressed. E-mail: liuwf@ustc.edu.cn, cfzhu@ustc.edu.cn, Tel.: +86-551-3602938, FAX: +86-551-3602940

thermal diffusion of sulfur and selenium vapors simultaneously into co-sputtered Cu-In alloy precursors is reported. The influence of heat treatments on in-depth composition distribution properties is investigated, and the reaction mechanism during heat treatments is also discussed.

II. EXPERIMENTS

Cu-In alloy films were co-sputtered from high purity Cu (5N) and In (5N) targets at ambient temperature onto glass or Mo-coated glass substrates using direct current (DC) sputtering and radio frequency (RF) sputtering, respectively. The background pressure was 50 μPa, and Ar sputtering pressure was 0.25 Pa. Alloy precursors with Cu/In ratio about 0.9 and thickness around 0.9 μm were achieved by co-sputtering Cu and In targets at 15 and 45 W respectively for 30 min.

Simultaneous thermal diffusion of S and Se vapor into the Cu-In alloy films was performed in a quasi-closed quartz crucible in a vacuum furnace with a background pressure of 1 Pa. As mentioned above, two kinds of reaction temperature profiles "one step profile" and "two step profile" were investigated. For "two step profile", the samples were annealed first at 250, 300, and 350 °C for 20 min then at 500 °C for 20 min. For "one step profile", the samples were annealed just at 500 °C for 20 min. The temperature of S/Se sources was 350 °C, and the added S/(S+Se) molar ratio in the quartz crucible was 0.05/1 while keeping the total mole number of S and Se powders 1 mmol.

The crystalline phases of the obtained thin films were characterized by X-ray diffraction (XRD, MXPAHF diffratometer with Cu Kα radiation, λ=1.5406 Å) and Raman spectra (LABRAM-HR micro-Raman system). The in-depth composition distribution was examined by grazing incident X-ray diffraction (GIXRD) and by energy dispersive spectrum (EDS) measurements as a function of the sample depth. The absorber layers were repeatedly etched in bromine methanol, followed by EDS measurements after each etching step. Chemical etching was conducted at room temperature in 1%Br_2/CH_3OH and the samples were rinsed in deionized water and blown dry with nitrogen before EDS measurements.

III. RESULTS AND DISCUSSION

A. Structure and in-depth compositional distribution analysis

The XRD results of $CuIn(S,Se)_2$ thin films by simultaneous sufo-selenization of co-sputtered Cu-In alloy precursors are shown in Fig.1. The XRD patterns indicate that the main phase in the annealed films is $CuIn(S,Se)_2$. $In_2(S,Se)_3$ appears only in the thin films annealed first at 250 °C for 20 min then at 500 °C for 20 min, which may be related to the large amounts of

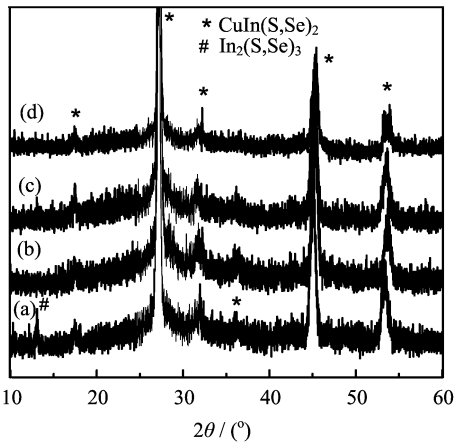

FIG. 1 XRD spectra of $CuIn(S,Se)_2$ thin films annealed first at (a) 250 °C, (b) 300 °C, (c) 350 °C for 20 min and then annealed at 500 °C for 20 min, respectively; and (d) annealed only at 500 °C for 20 min.

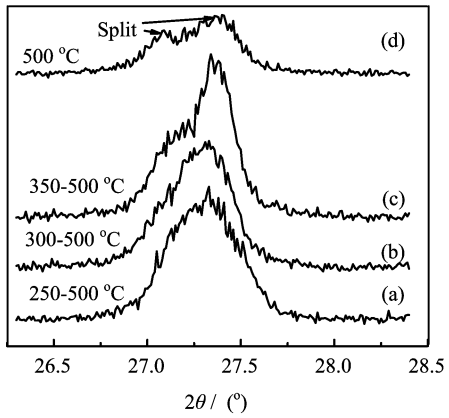

FIG. 2 Enlarged XRD (112) peak of $CuIn(S,Se)_2$ thin films annealed first at (a) 250 °C, (b) 300 °C, (c) 350 °C for 20 min and then at 500 °C for 20 min, respectively; and (d) annealed only at 500 °C for 20 min.

In-Se-S phase formed under 250 °C but not be consumed completely during 500 °C.

Figure 2 (a), (b) and (c) show the enlarged (112) peaks of film's XRD spectra annealed with "two step profile", while Fig.2(d) displays the (112) peaks of film's XRD spectrum annealed with "one step profile". It is noted that the symmetry of (112) peaks of $CuIn(S,Se)_2$ films becomes worse as the low temperature stage in "two step profile" increases. When the low temperature stage was removed, the (112) peak of $CuIn(S,Se)_2$ thin films annealed with "one step profile" at 500 °C splits.

The symmetry of (112) peaks is a structure proof for homogeneous $CuIn(S,Se)_2$ thin films. Peaks broadening or splitting is normally observed in graded or double phase materials [2]. In other words, the symmetry of (112) peaks is related to in-depth composition distribution, especially S/Se distribution of the $CuIn(S,Se)_2$ thin films. Thus it might infer that the thin films an-

DOI:10.1088/1674-0068/25/04/481-486

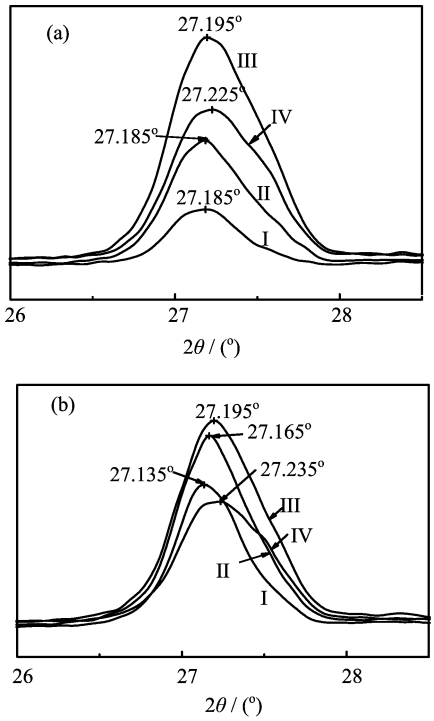

FIG. 3 Enlarged (112) peaks of GIXRD patterns of $CuIn(S,Se)_2$ thin films. (a) Sample A: first annealed at 250 °C for 20 min then annealed at 500 °C for 20 min. (b) Sample B: only annealed at 500 °C for 20 min. I, II, III, and IV represent the incident angle of 1°, 2°, 5°, and 10°, respectively.

nealed with "two step profile" have better in-depth compositional uniformity than that with "one step profile", and it seems that the low temperature stage in "two step profile" influences the diffusion behavior of elements during thermal annealing.

To further confirm the inference, GIXRD was carried out on these films. GIXRD is a kind of technique which use various fixed low incident angle in XRD. Various incident angle means different penetration depth, thus GIXRD can capture structure information coming from different depth of samples to assess the compositional homogeneity of the samples.

Figure 3 shows the enlarged (112) peaks of GIXRD spectra of thin typical films annealed with "two step profile" and "one step profile", respectively. For better illustration, we named sample A for samples annealed under "two step profile" and sample B for samples annealed at "one step profile". Incident angles of 1°, 2°, 5°, and 10° were employed. With the increase of the S/(S+Se) ratio in $CuIn(S,Se)_2$ thin film, the crystal lattice decreases, because S^{2-} has the smaller ion diameter compared with Se^{2-}. From Fig.3, it is clearly revealed that the (112) peak shifts to larger angle, which means that the S/(S+Se) ratio increases with the incident angel increasing. In GIXRD spectra, generally speaking, low incident angles (about <5°) represent information from the top surface of the thin films, while higher incident angles (5°−10°) represent information from the bulk region [7]. According to the above observations, from top surface to in-depth bulk region, the S content in the thin films increases as the depth increases. That is because S has much lower melting point (about 112 °C) than that of Se (about 217°C). As a result, the precursors first reacted with S vapor and then reacted with S/Se mixed vapor. S was partially substituted by Se gradually from top surface to bulk, which finally led to the S depth profile. When the incident angle changes from 1° to 10°, in Fig.3(a), the 2θ value of (112) peak shifts from 27.185° to 27.225°, the extent of 2θ value variable is 0.04°; while in Fig.3 (b), the 2θ value of (112) peak shifts from 27.135° to 27.235°, the extent of 2θ value variable is 0.1°. This indicates that compositional broadening of thin films is more severe in sample B than that in sample A. In other words, thin films annealed with "two step profile" have better in-depth compositional uniformity than that with "one step profile", which is consistent with the inference from Fig.2.

Bromine methanol has previously been used in the surface treatment of chalcopyrite thin films in order to remove damaged or poorly crystallized regions near the surfaces of the films [8]. Alberts *et al.* have achieved in-depth composition distribution curves of $CuInSe_2$, $Cu(In,Ga)Se_2$ and $CuIn(S,Se)_2$ through etching films in bromine methanol repeatedly, followed by measurements of the characteristic XRF $K_{\alpha 1,2}$ line intensities of the remaining layer after each etching step [9−12]. In our experiments, we used EDS instead of XRF measurements for convenience. It is important to realize that these compositional profiles represent the compositional features of the remaining material after successive etching steps. Figure 4 shows the in-depth composition concentration as a function of thickness of remaining absorber films after each etching step of sample A and sample B. The first four points in the dot lines on the right of the Fig.4 (a) and (b) represent the bulk element concentrations of the unetched samples. The initial thicknesses of these films were around 2.4 μm, which were etched down to a final thickness of around 0.4 μm.

We can see from Fig.4 that there is a drop in S content as a function of film thickness, corresponding to an increase in Se content as a function of film thickness. And chalcogen elements contents change slowly in top layer of absorber films while sharply in back layer, the thickness of the turning point is less than 1 μm. Comparing Fig.4 (a) with (b), it is clearly evident that there is a discrepancy on compositional distribution. The S/Se atomic ratio increases more fast in Fig.4(b) than that in Fig.4(a), especially in the top layer of absorber films, which indicates that the chalcogen elements distribution is more homogeneous in thin films annealed with "two step profile" than that with "one step profile". The data of S/(S+Se) ratio are shown in Table I, which prove the observation. For sample A, S/(S+Se) ratio changes from 0.46 to 0.59 when film thickness decreases

DOI:10.1088/1674-0068/25/04/481-486

TABLE I In-depth EDS data obtained from sample A and B repeatedly etched in bromine methanol.

Sample	Etching step	Film thickness/μm	Element concentration/%				S/(S+Se)
			Cu	In	S	Se	
A	0	2.3	23.84	30.21	21.24	24.71	0.46
	1	2.1	22.56	29.47	26.14	21.84	0.54
	2	1.8	21.31	27.82	28.43	22.44	0.55
	3	1.5	20.40	25.73	31.29	22.59	0.58
	4	1.1	19.97	23.29	33.87	22.87	0.59
	5	0.7	19.46	19.33	41.25	19.96	0.67
	6	0.3	0.65	19.14	80.21	0.00	1.00
B	0	2.4	21.99	32.28	11.45	34.29	0.25
	1	2.1	21.23	30.76	18.02	29.99	0.37
	2	1.8	20.93	31.41	22.88	24.78	0.48
	3	1.5	19.11	31.27	26.26	23.36	0.52
	4	1.2	17.77	28.25	29.44	24.54	0.54
	5	0.9	16.94	26.20	33.56	23.30	0.59
	6	0.5	12.10	11.15	67.02	9.74	0.87

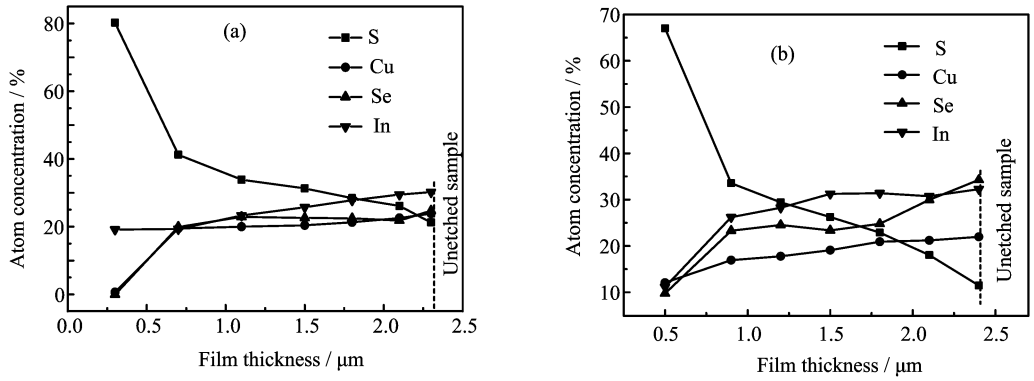

FIG. 4 The elements concentration of the samples etched in Br_2/CH_3OH as a function of film thickness. (a) Sample A: annealed first at 250 °C then at 500 °C. (b) Sample B: annealed only at 500 °C for 20 min.

from 2.3 μm to 1.1 μm, the variable is about 0.14. While for sample B, S/(S+Se) ratio changes from 0.25 to 0.54 when film thickness decreases from 2.4 μm to 1.2 μm, the variable is about 0.29.

Another interesting discrepancy between sample A and sample B is in the back layer of thin films. For sample A, In content remains high but Cu content experiences a sharp drop, while for sample B, In and Cu contents decrease simultaneously. This is in accordance with the XRD results from Fig.1 that the $In_2(S,Se)_3$ appears in sample A but not in sample B, maybe owing to quantities of In reacting with S/Se in the back layer of the thin films under 250 °C for sample A. Co-sputtered Cu-In alloy precursors is apt to the formation of CuSe on the surface of films and InSe in the bottom layer of films when selenized under 300 °C [13], so when sample A is sulfurized/selenized under low temperature, they may form Cu(S,Se) on the surface and In-S-Se in the bottom layer.

B. Reaction mechanism analysis

As mentioned above, the low temperature stage of "two step profile" may influence the diffusion behavior of elements during thermal annealing. To further figure out the reaction mechanism of the two thermal processing, the low temperature stage during "two step profile" was investigated. Three samples were annealed at 250, 300, and 350 °C for 20 min, respectively. Then the ohmic heating power supply was turned off according to automatic program and these samples were cooled down quickly to room temperature.

Figure 5 depicts XRD patterns of $CuIn(S,Se)_2$ thin films annealed at 250, 300, and 350 °C for 20 min respectively then cooled down to room temperature quickly. As the temperature increases, the XRD peaks of $CuIn(S,Se)_2$ become stronger and sharper, while the peaks of Cu(S,Se) become weaker, and at last disappear almost. InS phase appears at 250 °C, and transfers into In_2S_3 phase at 300 °C. In_2S_3 phase develops to be a

DOI:10.1088/1674-0068/25/04/481-486

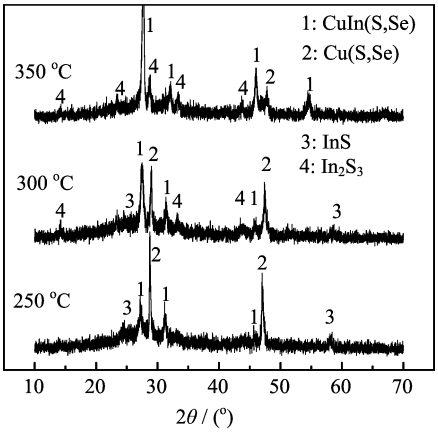

FIG. 5 XRD patterns of $CuIn(S,Se)_2$ thin films annealed at 250, 300, and 350 °C for 20 min respectively then cooled down to room temperature quickly.

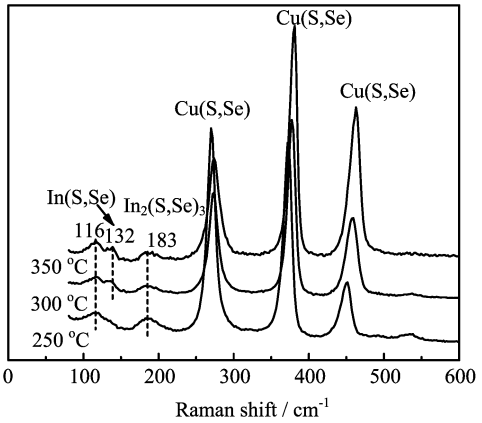

FIG. 6 Raman patterns of $CuIn(S,Se)_2$ thin films annealed at 250, 300, and 350 °C for 20 min respectively, then cooled down to room temperature quickly.

dominant In-S binary compound at 350 °C. This indicates that as the "low temperature stage" increases, the amount of $CuIn(S,Se)_2$ increases and the crystallinity of $CuIn(S,Se)_2$ gets better, corresponding to the consumption of Cu(S,Se) and In-S binary compounds. The peaks of $CuIn(S,Se)_2$ and Cu(S,Se) shift to higher 2θ value, which indicates the S/(S+Se) ratio increases in $CuIn(S,Se)_2$ and Cu(S,Se) phases as the temperature gets higher [5, 13]. The stronger reactivity of S than Se may be responsible for this observations. Although both the reactivity of the two elenments improves with elevated temperature, it seems that the reactivity of S increases even more fast. This results is similar to the experiment results of S/(S+Se)=0.25 reported by Hölzing *et al.* [14].

In Fig.5, almost no In(S,Se) and $In_2(S,Se)_3$ is presented, the corresponding peaks match well with InS (JCPDS No.05-1472) and In_2S_3 (JCPDS No.65-0459). Strictly speaking, at 350 °C, there is slightly blue shift of peak of In_2S_3, this indicates trace quantities of Se has diffused into In_2S_3 to form $In_2(S,Se)_3$. The results show that S element in InS and In_2S_3 can not be easily replaced by Se. In-chalcogens show a smaller solid solution range of Se and S due to no isostructural phases existing in the In-S/In-Se systems [14, 15]. The experiment results indicate that Se passing into $CuIn(S,Se)_2$ is mainly via Cu(S,Se) rather than In(S,Se) or $In_2(S,Se)_3$.

Raman spectra shows the crystalline phases in the top layer of thin films (see Fig.6). From 250 °C to 350 °C, there are large quantities of Cu(S,Se) phase on the surface of thin films. The peaks of Cu(S,Se) shift to the right side gradually. According to the reported results of Ishii *et al.* [16], the corresponding S/(S+Se) atomic ratio in Cu(S,Se) increases from about 0.4 to 0.67 when the temperature increases from 250 °C to 350 °C in these three samples. In addition, in Cu(S,Se) phase S/(S+Se) atomic ratio follows a linear relationship of XRD (112) peak position [17], so it can be calculated from XRD data that from 250 °C to 350 °C, S/(S+Se) is about 0.4−0.5, which is lower than the values calculated from Raman data especially at 350 °C. Raman spectra reflect information of top surface while XRD reflects information of the whole bulk, so this result provides a proof for the explanation that the reactivity of S is stronger than that of Se at the same temperature and increases more fast when temperature rises. Because the surface is directly exposed to S/Se vapors and more sensitive to S/(S+Se) than the in-depth bulk.

It is difficult to determine the In(S,Se) or $In_2(S,Se)_3$ phase through Raman spectra due to very few Raman studies reported on these two phases to my knowledge. Researchers reported that InSe films exhibited feature at 118 cm^{-1} [18, 19]. In view of the length of scan step of 2 cm^{-1} and severe broadening of the peak of 116 cm^{-1}, we assume the band at 116 cm^{-1} represents In(S,Se). Band of 134 cm^{-1} appears in ultra-thin InSe films [18], thus band of 132 cm^{-1} can be assigned to In(S,Se) as well. Peaks of 180, 182, 183 cm^{-1} present in β-In_2S_3, α-In_2Se_3, and γ-In_2Se_3 crystals respectively [20, 21], we cannot determine the phase of 183 cm^{-1} peak according to the known knowledge, so here we let $In_2(S,Se)_3$ for representative.

These In-S-Se phases may come from the diffusion of In-S in the bottom. The presence of CuSe and InSe in selenium-containing precursors is responsible for the improved in-depth compositional uniformity of $CuInSe_2$ thin films [9]. Thus Cu(S,Se) and In-S compounds may also promote the in-depth compositional uniformity of $CuIn(S,Se)_2$ thin films. It could be explained as follows. For better illustration, we denote that the "two step profile" includes a "low temperature stage" and a "high temperature stage". It is easy to know that there are two reaction routes for formation of $CuIn(S,Se)_2$ compound. On one hand, at temperatures below 350 °C, Cu(S,Se) and In-S compounds are formed in considerable amounts, when the temperature increases, Cu(S,Se) and In-S compounds will react to

DOI:10.1088/1674-0068/25/04/481-486

form $CuIn(S,Se)_2$. On the other hand, S and Se vapors can diffuse from the surface into bulk of thin films through competition, to form new $CuIn(S,Se)_2$ compound by changing the S/Se atomic ratio of the former formed $CuIn(S,Se)_2$ compound. These processes can be described by the following equations:

$$Cu(S,Se) + InS(In_2S_3) \rightarrow CuIn(S,Se)_2 \quad (1)$$

$$CuIn(S,Se)_2(\text{former}) + S/Se(\text{vapour}) \rightarrow CuIn(S,Se)_2(\text{new}) \quad (2)$$

These two reactions are also suggested in *in-situ* XRD results [15]. As the "low temperature stage" of "two step profile" is low, the quantity of Cu(S,Se) and In-S compounds is large, so in "high temperature stage" reaction (1) is dominant. As the "low temperature stage" becomes higher or "one step profile" is employed, the quantity of Cu(S,Se) and In-S compounds in the thin films decreases quickly, while $CuIn(S,Se)_2$ compound increases to be the main phase. So when the temperature rises to "high temperature stage", $CuIn(S,Se)_2$ compound is formed mainly through reaction (2). For reaction (1), there are large quantities of Cu(S,Se) on the surface of thin films, and at high temperature Cu(S,Se) is molten. As a result, S/Se can diffuse quickly into the thin films to form Cu(S,Se) with uniform S/(S+Se). The S concentration deceases quickly on the surface and due to concentration gradient, In-S in the bottom diffuses fast to the surface and reacts with Cu(S,Se) to form relatively uniform $CuIn(S,Se)_2$ thin film. For reaction (2), as the self diffusion coefficient of Se in $CuInSe_2$ is about 2×10^{-13} cm^2/s [22], it could be lower than the diffusion coefficient of Se in molten Cu(S,Se) by several orders of magnitude, so the concentration gradient of S should be lower than that in reaction (1). As a result, $CuIn(S,Se)_2$ thin films with poor uniformity are in S/Se distribution form. In a word, $CuIn(S,Se)_2$ thin films annealed with "two step profile" have better in-depth compositional uniformity than those annealed with "one step profile".

IV. CONCLUSION

$CuIn(S,Se)_2$ thin films were prepared by thermal crystallization of co-sputtered Cu-In alloy precursors in S/Se atmosphere. Thermal treatments have great effects on in-depth compositional uniformity of $CuIn(S,Se)_2$ thin films. The thin films show more homogeneous distribution of S/Se annealed with "two step profile" than that with "one step profile". Two reaction routes (see reaction (1) and (2)) for formation of $CuIn(S,Se)_2$ are presented to explain the mechanism during the thermal annealing process. When samples are annealed with "two step profile", reaction (1) is dominant. Amounts of Cu(S,Se) on top surface of thin films in reaction (1) promotes the S/Se interdiffusion, which leads to relatively uniform $CuIn(S,Se)_2$ thin films. When samples are annealed with "one step profile", reaction (2) is dominant. As Se diffuses much slower in $CuIn(S,Se)_2$ than that in molten Cu(S,Se) at elevated temperature, $CuIn(S,Se)_2$ thin films with poor in-depth uniformity of S/Se distribution finally form when annealed with "one step profile".

V. ACKNOWLEDGMENTS

This work was supported by the National Basic Research Program of China (No.2012CB922001) and the Fundamental Research Funds for the Central Universities (No.WK2060140005).

[1] P. Jackson, D. Hariskos, E. Lotter, S. Paetel, R. Wuerz, R. Menner, W. Wischmann, and M. Powalla, Prog. Photovolt Res. Appl. **19**, 894 (2011).
[2] C. J. Sheppard and V. Alberts, J. Phys. D **39**, 3760 (2006).
[3] S. Bandyopadhyaya, S. Roy, S. Chaudhuri, and A. K. Pal, Vacuum **62**, 61 (2001).
[4] T. Yamaguchi, M. Nakashima, and A. Yoshida, *3rd World Conference on Photovolraic Energy Conversion*, Osaka, Japan, May 11-18, (2003).
[5] T. Yamaguchi, T. Naoyamaa, H. S. Leeb, A. Yoshidab, T. Kobatac, S. Niiyamac, and T. Nakamurac, J. Phys. Chem. Solids **64**, 1831 (2003).
[6] F. O. Adurodija, J. Song, I. O. Asia, and K. H. Yoon, Solar Energy Mater. Solar Cells **58**, 287 (1999).
[7] Y. Q. Lai, S. S. Kuang, F. Y. Liu, Z. X. Yuan, Z. A. Zhang, Y. Li, J. Liu, B. Wang, D. Tang, J. Li, and Y. X. Liu, Appl. Surf. Sci. **257**, 8360 (2011).
[8] R. Klenk and H. W. Schock, *Proceedings of the 10th IEEE Photovoltaic Specialists Conference*, Lisbon, 927 (1992).
[9] V. Alberts and M. L. Chenene, J. Phys. D **32**, 3093 (1999).
[10] V. Alberts, Jpn. J. Appl. Phys. **41**, 518 (2002).
[11] V. Alberts, M. Klenk, and E. Bucher, Solar Energy Mater. Solar Cells **64**, 371 (2000).
[12] J. Bekker, V. Alberts, A. W. R. Leitch, and J. R. Botha, Thin Solid Films **431-432**, 116 (2003).
[13] V. Alberts, Thin Solid Films **517**, 2115 (2009).
[14] A. Hölzing, R, Schurr, S, Jost, Jörg Palm, Klaus Deseler, P. J. Wellmann, and R. Hock, Mater. Res. Soc. Symp. Proc. **1165**, M02 (2009).
[15] A. Hölzing, R. Schurr, H. Schäfer, A. Jäger, S. Jost, J. Palmb, K. Deseler, P. Wellmann, and R. Hock, Thin Solid Films **517**, 2213 (2009).
[16] M. Ishii, K. Shibata, and H. Zozaki, J. Solid State Chem. **105**, 504 (1993).
[17] H. Nozaki, K. Shibata, and M. Ishii, J. Solid State Chem. **118**, 176 (1995).
[18] S. Shigetomi and T. Ikari, Jpn. J. Appl. Phys. **30**, 2127 (1991)
[19] R. Schwarcz, M. A. Kanehisa, M. Jouanne, J. F. Morhange, and M. Eddrief, J. Phys.: Condens. Matter **14**, 967 (2002).
[20] K. Kambas, C. Julien, M. Jouanne, A. Likforman, and M. Guittard, Phys. Stat. Sol. (b) **124**, K105 (1984).
[21] R. Lewandowska, R. Bacewicza, J. Filipowicz, and W. Paszkowicz, Mater. Res. Bull. **36**, 2577 (2001).
[22] V. Bardelebena, J. Appl. Phys. **56**, 321 (1984).

DOI:10.1088/1674-0068/25/04/481-486